metals

MDPI

Article

Effect of Fly Ash Addition on the Physical and Mechanical Properties of AA6063 Alloy Reinforcement

Alaa Mohammed Razzaq [1,2], Dayang Laila Majid [1,*], Mohamad R. Ishak [1] and Uday M. Basheer [3,4]

1 Department of Aerospace Engineering, Faculty of Engineering, Universiti Putra Malaysia, 43400 UPM Serdang, Selangor Darul Ehsan, Malaysia; alaaupm@gmail.com (A.M.R.); mohdridzwan@upm.edu.my (M.R.I.)
2 Oil Products Distribution Company, Iraq Ministry of Oil, 10022 Al Doura, Baghdad, Iraq
3 Faculty of Mechanical Engineering, Universiti Teknologi Malaysia, 81310 Johor Bahru, Johor, Malaysia; uday@utm.my
4 UTM Centre for Low Carbon Transport in Cooperation with Imperial College London, Institute for Vehicle Systems and Engineering, Universiti Teknologi Malaysia, 81310 Skudai, Malaysia
* Correspondence: dlaila@upm.edu.my; Tel.: +60-133-818-377; Fax: +60-386-567-125

Received: 12 September 2017; Accepted: 18 October 2017; Published: 4 November 2017

Abstract: Aluminum-fly ash particulate-reinforced composites (AA6063-FA) have been used in various engineering fields, such as automotive and aerospace industries, due to their low density and good mechanical properties. There are many fabrication techniques available to manufacture these composites according to matrix and reinforcement materials. The compocasting technique for the fabrication of the AA6063 matrix composite reinforced with fly ash particles is the focus of this research. Fly ash content was in the range of 0–12 wt % in increasing increments of 2%. Fly ash particles were added to the molten AA6063 alloy until they were completely blended and cooled down just below the liquidus to keep the slurry in the semi-solid state. After this, the molten AA6063-FA composites were cast into prepared cast iron molds. Bulk density and apparent porosity measurements, Charpy impact testing, Vickers microhardness measurements, Field Emission Scanning Electron Microscope (FESEM), Variable Pressure Scanning Electron Microscope and Energy Dispersive X-ray spectroscope (EDS) elemental mapping were used to evaluate these materials. The results showed that an increase in the fly ash content in the melted leads results in an increase in the microhardness and porosity in the composites. In contrast, the bulk density and Charpy impact energy of the composites decreased with an increase in the fly ash content.

Keywords: aluminum composites; fly ash; porosity; casting; impact evaluation; microhardness

1. Introduction

The 6XXX series of aluminum alloys have so far exhibited remarkable mechanical properties, formability, higher corrosion resistance, better weldability, high strength-to-weight ratio and a lower cost as compared to other counterparts, such as the 2XXX and the 7XXX Al alloys. This set of aluminum alloys constitutes the highest volume of aluminum products, which have been widely employed in a variety of technologies, including automobile and aerospace industries, pipes, architectural applications, bicycle frames, transportation equipment, bridge railings and welded structures. Among the vast variety of alloying elements available for the development of the heat-treatable 6000 series, recent investigations have proposed silicon and magnesium as the major alloying elements. Moreover, both elements are essential materials for precipitate strengthening [1–4]. Furthermore, aluminum

AA6063 alloy is widely employed for construction and transportation applications [5]. As a baseline material, it possesses good formability, weldability, machinability and corrosion resistance as well as a medium strength relative to other grades of aluminum alloys [6,7]. However, with a view of implementing them as high performance materials for use in the aerospace, automobile, chemical and transportation industries, it is essential to improve the strength, elastic modulus and wear resistance of the AA6063 alloy compared to the conventional base [8].

Metal matrix composites (MMCs) is a macroscopic combination of two or more different materials (one of them is a metal and the other a non-metal) in which tailored properties are determined [9]. In recent years, the metal matrix composites have received considerable attention due to their low density, high strength and stiffness as compared to those of conventional materials [10]. The adhesive strength between the matrix and reinforcement plays an important role in the determination of mechanical properties for MMCs [11,12]. Many researchers have discussed these aspects. Reinforcement particles incorporated into molten aluminum were observed to possibly guarantee the production of components with decent functional capacities in mechanical, structural and tribological applications [13–15]. Reinforcement is usually composed of non-metal components and generally conventional ceramic materials, such as SiC, Al_2O_3, fly ash and so on. Many important automotive components, such as pistons, cylinders, engine blocks, brakes, drive shafts and snow tire studs, have used aluminum matrix composites in their production. The new aluminum matrix composite engine has provided a higher compactness with great weight reductions compared with traditional engine blocks and those fabricated in aluminum alloys with other metal alloy liners, which thus provides a higher level of performance [16].

There are several fabrication techniques available to manufacture the MMC materials, such as casting, powder metallurgy and diffusion bonding. There is no unique way in this regard. Due to the choice of matrix and reinforcement as well as the relevant type of these materials, the fabrication techniques can vary considerably. The casting technique has received great attention in the last few decades for the fabrication of aluminum alloy components for different applications. The stir casting technique has proven to be the most promising technique amongst other liquid state production techniques. Sozhamannan et al. [17] investigated the influence of stir casting process parameters on the metal matrix composites. They showed that the reinforcement particles (SiC) are uniformly distributed in the aluminum matrix at the processing temperatures of 750 and 800 °C. The microhardness values increase with an increase in the temperature from 750 to 800 °C after 20 min of holding time. In addition, the impact energy values of aluminum matrix composites mainly depend on the distribution of the SiC particles in the matrix. The impact strength values are slightly increased with an increase in temperatures (700–900 °C). Khosravi et al. [18] studied the influence of the compocasting process parameters on the microstructure and mechanical properties of A356-SiC composites. Their results showed that uniformity in the SiC particle distribution was improved by increasing the stirring time and decreasing the stirring temperature. However, by increasing the stirring speed, the homogeneity first increases and then declines. In addition, they observed that the porosity of MMC increases by increasing the stirring speed, stirring time and temperature.

Among various reinforced ceramic materials used, fly ash is one of the most cheaper and low-density reinforcement material available as a solid waste byproduct during combustion of coal in thermal power plants. The chemical composition of this ash consists of Al_2O_3, SiO_2 and Fe_2O_3 as major constituents and MgO, CaO, K_2O and Na_2O as minor constituents [19–21]. The utilization of aluminum matrix composites with fly ash particles as reinforcement are likely to overcome the cost barrier for widespread applications, such as engineering, automotive and other applications. Many researchers have carried out various studies on the physical and mechanical properties of the aluminum matrix composites using fly ash as reinforcements [22–28]. For example, Selvam et al. [22] have studied the microstructure and mechanical properties of the AA6061 aluminum alloy reinforced with fly ash. The aluminum composites in this research were characterized as having homogeneous dispersion of fly ash particles with good bonds and a clear interface with the AA6061 aluminum

matrix. The incorporation of fly ash particles with the aluminum matrix improved the wettability and mechanical properties, such as microhardness. Shanmughasundaram et al. [19] investigated the utilization of fly ash with pure aluminum to produce composites by a two-step stir casting method. They showed that the density of the aluminum composites decreased with an increase in fly ash reinforcement content. The mechanical properties of these composites, such as microhardness, increased with an increase in fly ash content. Mahendra and Radhakrishna [10] have produced hybrid aluminum copper alloy composites with different weights of fly ash and SiC particles. The hybrid composite was tested for fluidity, hardness, density, impact strength and other mechanical properties. The results show that there is an increase in hardness, impact strength and other mechanical properties with an increase in the content of particulates. In contrast, the density decreases with an increase in the content of fly ash and SiC. Gikunoo et al. studied the influence of adding fly ash on the mechanical properties of 535 aluminum casting alloy. The results show that the increasing fly ash content of the aluminum composite increased the brittleness and porosity of the casted samples, which affected and decreased Charpy impact strength of aluminum/fly ash composites [29].

The aim of this investigation is to elucidate the effect of fly ash addition on the microstructure, physical and mechanical properties of the AA6063 alloy. The casting processes were carried out by using compo-casting technique. Properties, such as bulk density, apparent porosity, Charpy impact testing and Vickers microhardness measurements, were investigated and the relationship of these properties with microstructure characterizations have been presented and discussed.

2. Materials and Methods

2.1. Materials

The metal alloy used in this study was AA6063 alloy supplied by a local supplier (Kamco Aluminium Bhd., Kuala Lumpur, Malaysia) as the matrix alloy. The elemental compositions of AA6063 alloy determined by the Wavelength Dispersive X-ray fluorescence (WDXRF) technique (Bruker S8; Tiger, Billerica, MA, USA) are shown in Table 1. The fly ash was obtained from Tanjung Bin Power plant in Pontian, Johor, Malaysia. The chemical composition of the fly ash is given in Table 2. The fly ash should be initially dried by oven (Memmert, Schwabach, Germany) at 100 °C for 48 h in the laboratory. The fly ash was then crushed and grounded to reduce the size of aggregated lumps into fine powders, which were finally passed through a 44-µm screen (325 Mesh). The particle size analysis was measured using a Malvern particle Mastersizer (Malvern Instruments Limited, Malvern, UK). Afterwards, the fly ash particles were preheated at the temperature of 900 °C for 2 h in order to remove the organic and inorganic impurities, water content and improve the wettability of the reinforcement particles with AA6063 alloy.

Table 1. Chemical composition of tested AA6063 in wt %.

Elements	Cu	Fe	Mg	Mn	Si	Ti	Zn	Cr	Al
wt %	<0.01	0.19	0.51	0.04	0.86	0.008	0.01	0.01	Balance

Table 2. Chemical composition of fly ash (FA) in wt %.

Elements	SiO_2	Al_2O_3	Fe_2O_3	TiO_2	K_2O	CaO	MgO	Na_2O	CuO
wt %	59.98	19.09	2.78	1.14	1.09	0.63	0.38	0.34	0.01

2.2. Casting Process

Stir casting is a cost-effective process for making aluminum matrix composites. There are several parameters in this process that influence the effect of the final microstructure and mechanical properties of the composites, such as preheated temperature of reinforcement and stirring time, on the uniform distribution of fly ash particles and resulting mechanical properties, such as microhardness and

impact behavior [17]. In this study, AA6063 alloy was melted in the induction furnace (Inductotherm Group, Seaford, Australia) integrated with the mechanically mixing stirrer (IKA, Brisbane , Australia), as shown in Figure 1. The AA6063 alloy was charged into the graphite crucible and heated to approximately 750 °C until the entire metal in the crucible was melted. The stainless-steel stirrer was lowered into the melt slowly to stir the molten AA6063 alloy at a speed of 300 rpm. The viscosity of the AA6063 alloy melt was maintained at the level to be just suitable for stirring and casting. The fly ash powder with particle sizes less than 44 μm was preheated at 800 °C for 2 h and added gradually to the melt with continuous stirring for 25–60 min. The melts of various percentages of fly ash particles (0–12 wt % in increasing increments of 2%) were cast as ingots in rectangular block-shaped molds with the dimensions of 200 × 65 × 23 mm^3. The samples were then cut and machined using a computer numerical control (CNC) Sodick AQ537L Wire-cut electrical discharge machining (EDM) machine tool (Sodick, Schaumburg, IL, USA) with hard brass wire of 0.25 mm diameter to organize it into suitable sizes for characterizations. After this, the cast test samples were treated with heat for 2 h at 560 °C, quenched in water at room temperature and then aged for 3 h at 160 °C.

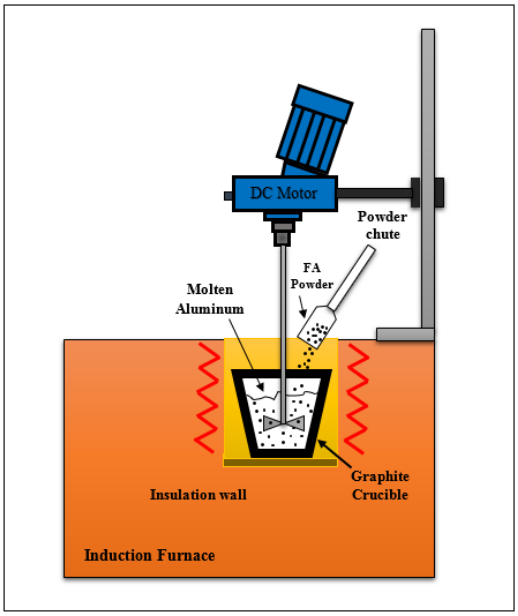

Figure 1. Schematic diagram of casting technique (DC: Direct current; FA: Fly ash).

2.3. Microstructure Observation

The casting composites samples used for microstructure observation were cut into rectangular bars with dimensions of 10 × 10 × 5 mm^3 using a low-speed diamond saw. The cross-sections of these samples were ground with 400–1200 grit silicon carbide papers, polished using 2 μm alumina paste as final polish and then cleaned with acetone bath. The composite samples were etched using a Keller's reagent, which consists of 2 mL HF (48%), 3 mL HCl (37%) and 5 mL HNO_3 (65%) in 190 mL of distilled water. The microstructure of these samples was observed using Field Emission Scanning Electron Microscopy (FESEM; HITACHI SU8020, Tokyo, Japan), Variable Pressure Scanning Electron Microscope (JEOL JSM-IT300LV, Akishima, Japan) and Energy Dispersive X-ray spectroscope (EDS; JEOL JSM-IT300LV, Akishima, Japan) for elemental mapping. All composite samples were platinum-sputtered prior to the observation.

2.4. Mechanical Characterization

Impact tests were designed to simulate the response of a material to a high rate of loading and involve a test piece being struck with a sudden blow [30]. The composite specimens for the impact

strength test were obtained in accordance with ASTM E23 standard using specimens with dimensions of 55 × 10 × 10 mm^3. The specimens had a V-shaped notch in the middle, with 0.25 mm root radius and 2 mm depth. Impact strength was obtained in a Charpy type impact test device (Gunt W400, Barsbüttel, Germany). The experimental tests were performed on five test samples for every percentage of fly ash added to AA6063 alloy. According to this test, the pendulum swings down from a specified height (h_o) to hit the composite test sample and fracture it. The height (h) to which the pendulum rises. After striking and breaking, energy used in the breaking is measured. If no energy were used, the pendulum would swing up to the same height (h_o) where it started from. Thus, the potential energy E_p at the top of the pendulum swing before and after the collision would be the same. A larger amount of energy used to break the test sample would result in a greater loss of energy and a lower height to which the pendulum rises. If the pendulum swings up to a height (h) after breaking the test sample, the energy used to break will be different between two heights ($E_p(h_o) - E_p(h)$). The energy E (J) required for breaking the test sample shall be obtained by the following formula [31]:

$$E = W \times g \times R \times (\mathrm{Cos}\beta - \mathrm{Cos}\alpha) \quad (1)$$

where W is weight of pendulum (Kgf); g is gravitational acceleration (m/s^2); R is distance from axis of rotation to center of gravity of pendulum (m); α is angle of fall of pendulum; and β is the angle of rise of pendulum in its swing after breaking test sample.

Microhardness testing using conventional Vickers hardness measurements was performed on AA6063-FA composite samples at different locations according to ASTM E 384. At least 10 Vickers type indents were performed on polished cross-section samples with a force of 4.9 N (0.5 kgf) and a holding time of 10 s by means of a Wolpert Group, Micro-Vickers Hardness Tester digital auto turret, Mod. 401MVD. Using a load-indenting microhardness tester (Wolpert Group, Schwabbach, Germany), the hardness was more closely measured, taking measurements every 0.3–0.5 mm. After the diagonal length measurement, the values of the Vickers hardness were calculated by the following equation:

$$H_V = 1.8544 \times \frac{F}{d^2} \quad (2)$$

where H_V is the Vickers hardness of composite samples; F is the applied load (kgf) and d is the arithmetic mean of the two diagonals, d_1 and d_2 (mm).

Following the mechanical tests applied to all the AA6063-FA composites, the fractured surfaces were examined under Variable Pressure Scanning Electron Microscope (VP-SEM JSM-IT300; JEOL, Akishima, Japan) to understand the fracture mechanism in AA6063-FA composites. The effect of various amounts of fly ash on changing the ductility or toughness of the composite could be followed using the VP-SEM.

3. Results and Discussion

3.1. Fly Ash (FA) Characteristics

The fly ash particle size, shape and distribution plays a vital role in determining the physical properties of the aluminum metal matrix composites. Figure 2 shows the results of the particle size analysis for fly ash powder used in this study. The average particle size of the fly ash powder is 21.96 μm, with the lower and higher values of 3.164 and 54.18 μm respectively, which are (10%) and (90%) of the fly ash particle size. Moreover, the particle size analysis calculated the density and specific surface area of the fly ash, which were found to be 2.33 g/cm^3 and 0.614 m^2/g, respectively.

The fly ash used in this research has been studied by the X-ray diffraction (XRD) technique using Rigaku XRD diffractometer (Rigaku Co., Akishima-shi, Japan) with Cu-Kα radiation (λ = 0.15406 nm). The data were collected from 2θ = 10–90° at a scan rate of 5°/min. The main components present in fly ash were found to be Mullite (90.5%), followed by Quartz (9.5%). The relative intensities in XRD peaks of fly ash matched the two references codes: Mullite (98-008-0147) and Quartz (98-010-7202).

The analysis of X-ray diffraction pattern results is shown in Figure 3. The relevant parameters corresponding to the diffraction peaks in the diagram have been computed by the X' Pert HighScore Plus software (version 3.0e, Amelo, The Netherlands) (Table 3). In addition, the morphology of the fly ash (Figure 4) shows that the fly ash particles are a spherical shape with a wide size distribution of particles and smooth surfaces. There are also some non-spherical and non-uniform particles present in Figure 4. The chemical analysis of the fly ash particles enabled by SEM-EDS elemental mapping typical results are shown in Figure 5. According to the results, the fly ash particles were found to contain significant quantities of O, Si, Al and Fe and trace amounts of K, Ti and Ca.

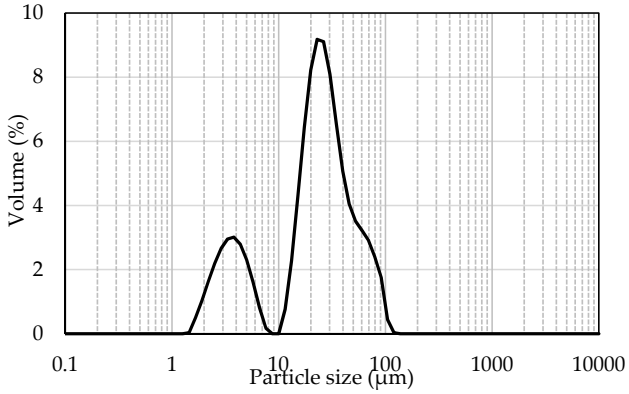

Figure 2. Particle size distribution of fly ash.

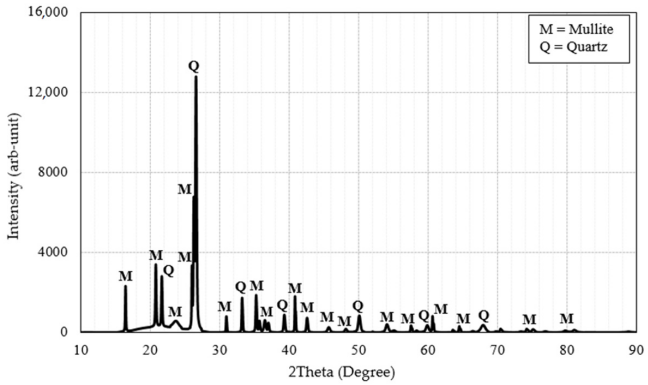

Figure 3. XRD diffraction pattern of fly ash calcined at 800 °C for 2 h (XRD: X-ray diffraction).

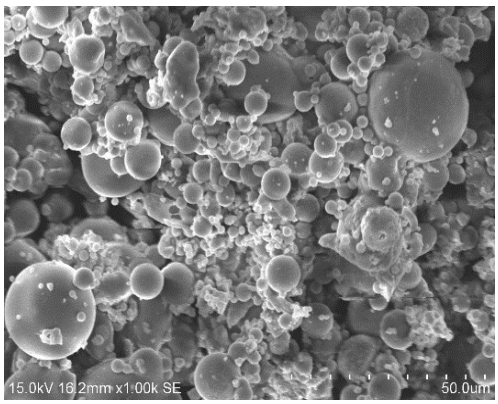

Figure 4. FESEM (Field emission scanning electron microscope) micrograph showing the morphology of fly ash particles.

Table 3. Relevant parameters of fly ash from XRD.

Chemical Name		Mullite	Quartz
Chemical formula		$Al_{4.64}O_{9.68}Si_{1.36}$	$O_{6.00}Si_{3.00}$
Crystal system		Orthorhmbic	Hexagonal
Crystallite size (Å)		27.9	311.8
Density calculated (g/cm^3)		2.37	2.23
Formula mass (g/mol)		318.27	180.25
Volume of cell (10^6 pm^3)		222.75	134.52
Space group		P b a m	P 31 2 1
Lattice parameters	a (Å)	7.93	5.27
	b (Å)	10.51	5.27
	c (Å)	2.675	5.59
	α (degree)	90	90
	β (degree)	90	90
	γ (degree)	90	120

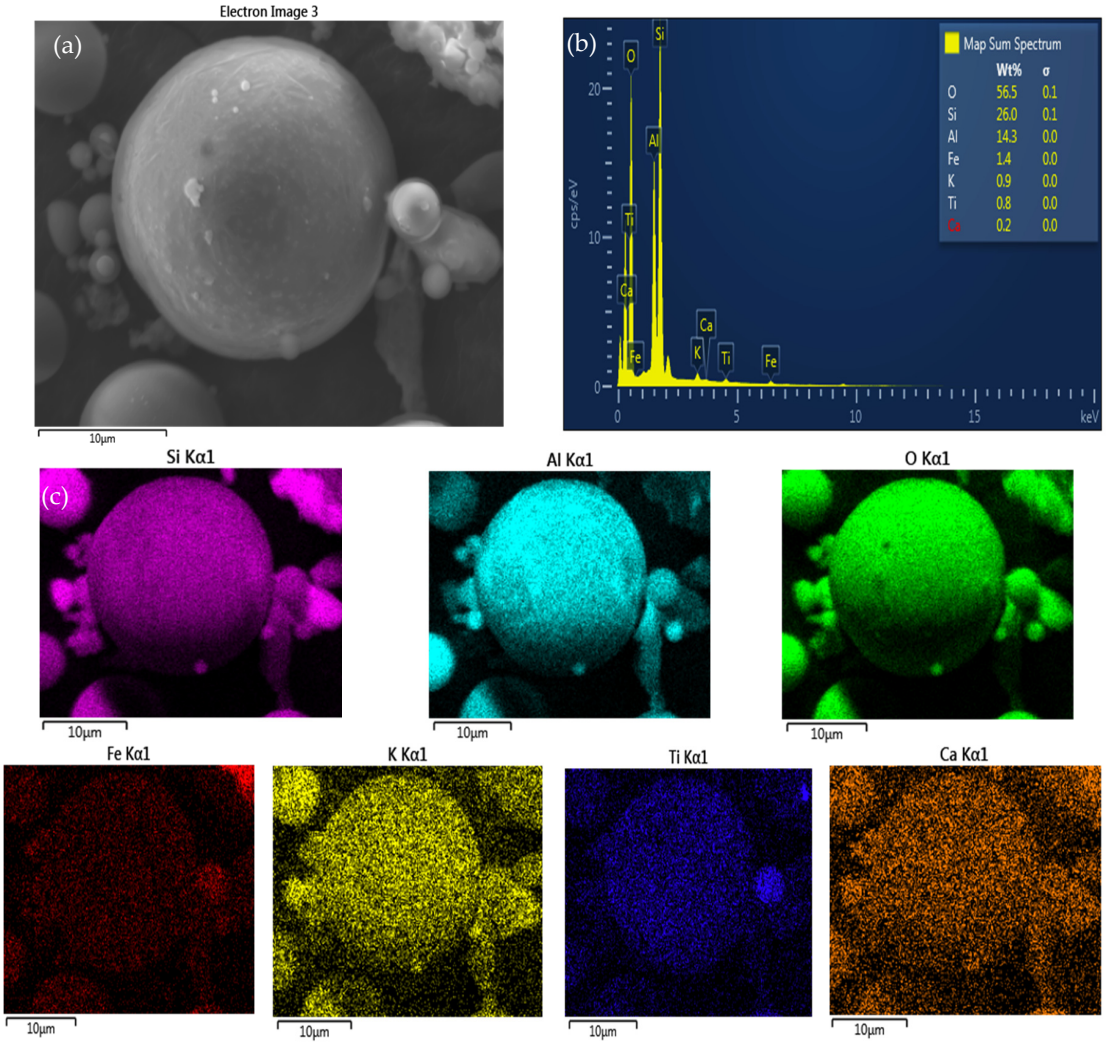

Figure 5. EDS (Energy dispersive X-ray spectroscope) elemental mapping of the raw fly ash powder: (**a**) SEM (Scanning electron microscope) image; (**b**) EDS spectrum of fly ash; and (**c**) corresponding elemental mapping of Si, Al, O, Fe, K, Ti and Ca, respectively.

3.2. AA6063-FA Composite Characteristics

3.2.1. Microstructural Characterization of AA6063-FA Composites

The VP-SEM micrographs of AA6063 alloy composites reinforced with fly ash are shown in Figure 6a,b. The micrographs of AA6063-FA composites show that the fly ash particles are uniformly distributed in the matrix, with no voids or defects observed. There was a good distribution between the fly ash particles and matrix material as well as very low agglomeration of fly ash in the low percentage content (Figure 6b). However, the problems of fly ash particle agglomeration and defects rapidly increase with an increase in the fly ash content. These problems will be discussed in the next few sections.

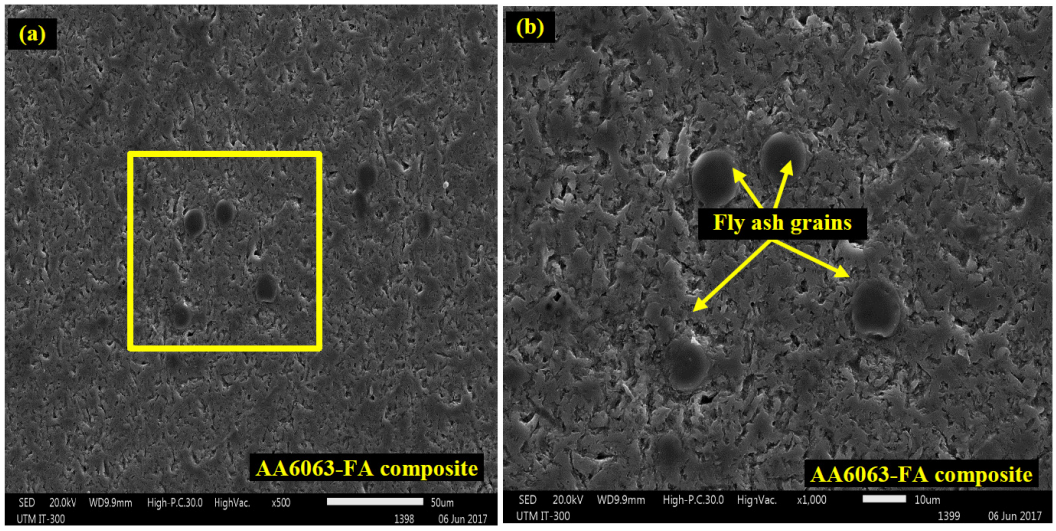

Figure 6. The microstructure of the AA6063-FA composite with 6 wt % fly ash observed under VP-SEM: (**a**) Fly ash grains in the surface at 500× and (**b**) 1000×.

3.2.2. Density and Porosity Measurements of AA6063-FA Composites

The bulk density and apparent porosity measurements of the cast AA6063-FA composite samples with different weight percentages of fly ash were determined by the Archimedes' method with water as the immersion medium. The variation of density and porosity of composites with different fly ash content samples is demonstrated in Figure 7. It can be observed that the bulk density values decrease and the porosity increases with an increase in reinforced fly ash particles. Since the density of fly ash (2.33 g/cm^3) is less than the density of AA6063 alloy (2.69 g/cm^3), the overall density of the AA6063-FA composites is reduced by increasing the amount of porosity in the casting conditions. Changes in the fly ash content cause a high amount of porosity being formed in composites.

It is encouraging that the percentage porosities are within the acceptable range of less than of 4% as reported in literature [32–34], which reported that a porosity of 4% is the maximum permissible value in cast metal matrix composites. The increased porosity of cast aluminum composites with increased fly ash content have also been reported by other researchers [29,35,36]. The porosity formation in the composites can be attributed to the increased content of the fly ash particles, which can lead to an increase in the porosity percentages of samples. This is due to several factors, one of which explains this increase in the levels of hydrogen gas that surround fly ash particles due to a sudden decrease in gas solubility during solidification [37,38]. After solidification is complete, these gas bubbles become micropores inside these samples. When these pores begin to form, the pores will grow until they reach a balance between several forces, including pressure, interfacial energy and hydrogen solubility. Furthermore, it was observed that reinforcing particles had a tendency to bind themselves sparsely [39],

leading to the formation of groups of pores (Figure 8). Other factors that influence the increase in the porosity of composites was insufficient to explain the gaps between adjacent ash particles due to expected increases in the effective viscosity of casting melts resulting in a higher gas holdup [40] and improper feeding of liquid metal [37]. Furthermore, there were increasing numbers of heterogeneous pore nucleation sites inside composite structures [41,42]. These types of porosity defects were usually found to be connected with groups of fly ash particles and they were rarely observed in the matrix surface when there are samples with a high content of fly ash (12 wt %; Figure 8). The porosity levels of cast composites were measured and chosen to be in the range of 2–4%. These porosity levels were slightly elevated due to the composite slurries still having gas and the casting having been carried out in the open atmosphere but could be considered reasonable due to casting conditions [29,43,44].

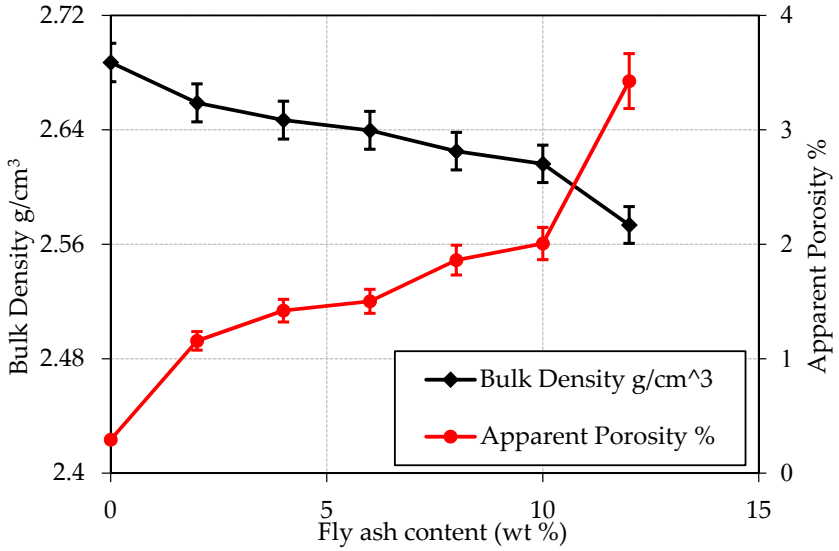

Figure 7. Bulk density and apparent porosity of AA6063-FA composites as a function of fly ash percentage content.

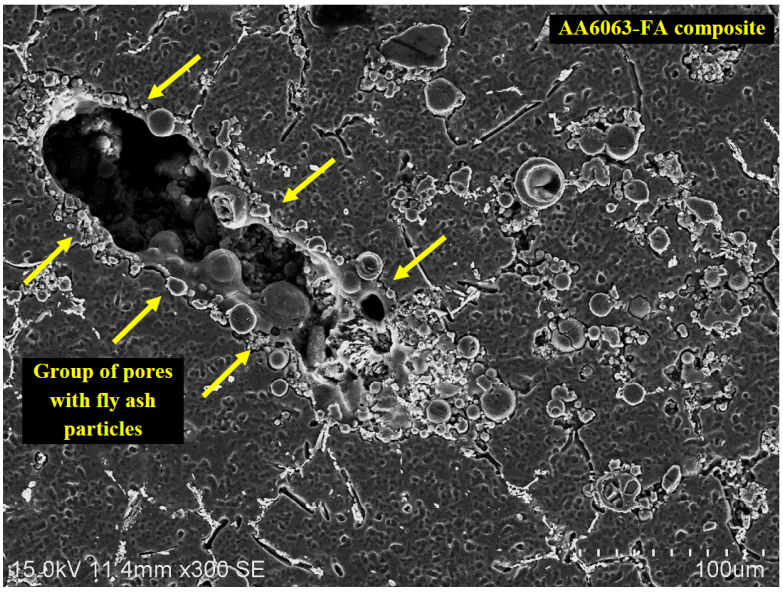

Figure 8. VP-SEM (Variable pressure scanning electron microscope) micrograph of the fly ash grains with group of pores in the surface of AA6063-FA composite (12 wt % fly ash).

3.3. Mechanical Properties of AA6063-FA Composites

The influence of changes in the weight percentage of fly ash added to AA6063-FA composites can be analyzed by determining the mechanical behavior of these composite samples subjected to different types of tests. The effect of including the fly ash powder in AA6063 alloys can be studied by conducting standard mechanical tests on the samples. In this study, the composite samples with different fly ash content are analyzed using two important mechanical properties, such as Charpy impact testing and microhardness measurements.

The Charpy impact test was conducted to determine the amount of energy absorbed by the AA6063-FA composites during fracture. Figure 9 shows the variation of Charpy impact energy with an increase in fly ash weight content (0–12 wt %). It can be seen that the energy absorbed in fracturing the composite samples decreased with an increase in fly ash content. In addition, a significant difference in Charpy impact strength exists between the casted AA6063 alloy and AA6063-FA composites. It is observed that the value of Charpy impact strength is higher in pure AA6063 alloy samples (15.1 J) compared with other percentages of fly ash content composites. The amount of energy absorbed during fracture decreased steeply with an increased percentage of the fly ash particles in the AA6063 alloy [45]. The addition of fly ash percentage (more than 2 wt % fly ash content) increases the brittleness and creates more groups of particle pores (Figure 8). This is due to the brittle nature of the reinforced fly ash particles, which reduced deformation capability and the ductility of the metal composites [46]. This increase in particulate and defects decreases the impact strength of AA6063-FA composites. The fly ash particles reinforcements act as obstacles for dislocating motions, which is needed for plastic deformation of the AA6063 matrix. The plasticity of the AA6063 composite will decrease when fly ash is added. Therefore, whenever they use fly ash reinforcements in ductile AA6063 alloy matrices, a decrease in the toughness is inevitable. The impact properties of particulate composites also depend on the interfacial adhesion between the reinforcement and the matrix [45].

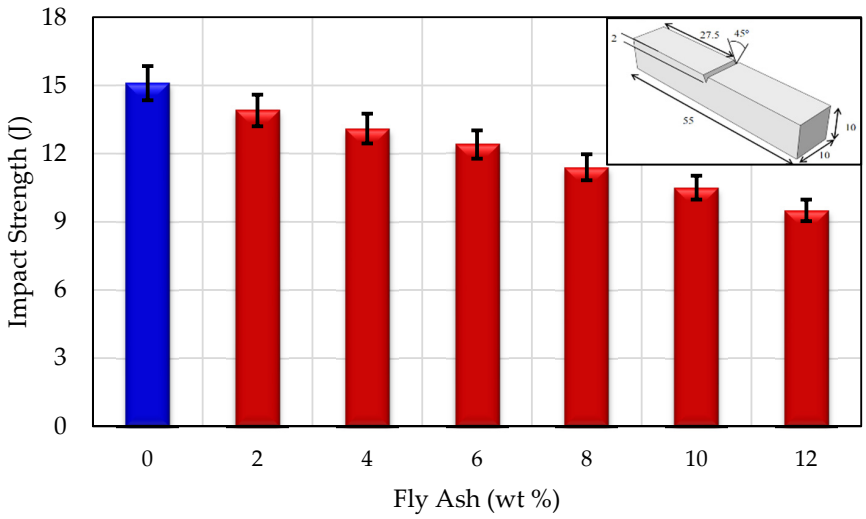

Figure 9. Charpy impact energy of AA6063-FA composites as a function of fly ash percentage content (All dimensions in mm).

The results of Vickers microhardness tests are shown in Figure 10. For AA6063-FA composite materials containing two different materials (soft metal matrix and fly ash particulates reinforcement), the selection of region to be collected in the surface sample for evaluating the microhardness data is very crucial in the case of particle-reinforced composites. Therefore, soft matrix, hard reinforcing phase and defects areas should be avoided in order to obtain the average microhardness from these tests. It is clear from Figure 9 that the Vickers microhardness results of the AA6063-FA composites is higher than that of the pure AA6063 alloy. The higher microhardness values of the composites could

be attributed to the fact that these reinforcements act as problems to the motion of dislocation [47]. The hardness of composite depends on the hardness of the reinforcements and matrices. The presence of silica and mullite in abundance increases the brittleness and hardness of aluminum composites when more reinforcement of fly ash is added as demonstrated in the XRD results (Figure 3).

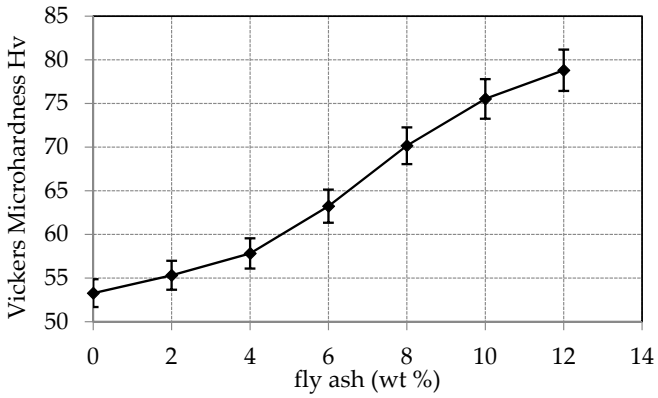

Figure 10. Vickers microhardness of AA6063-FA composites as a function of fly ash percentage content.

4. Fractography

Typical VP-SEM micrographs of Charpy impact fracture surfaces for different cast samples are shown in Figures 11–13. These images of fractography reveal some important differences in the appearance of the fractured impact AA6063-FA surfaces with respect to the level of reinforcement. The fracture surface of AA6063 alloy without additional fly ash is characterized by the presence of colonies in dimples of varying shapes and sizes, which is an indication that the failure in metal is the result of ductile fracture (Figure 11). Increasing the fly ash content resulted in a brittle fracture appearance, coupled with clearly defined dimples as shown in Figure 12. The proportion of grains (broken or unbonded) appear on the fracture surface with an increase in fly ash grain content as shown in Figure 13. It was noted for AA6063-FA composite that the grains occupied a higher proportion of the fracture surface than expected from their fly ash content. This was confirmed by comparing the number of grain agglomeration observed in a section through the crack path with the number intersected by an arbitrary straight line through the composite samples. According to the fractographic analysis just presented, the fracture of composite samples can be described as having disabilities for cohesive strength. However, in the case of AA6063-FA composites, the impact strength was decreased according to increase the fly ash concentration through the fracture region (Figure 13).

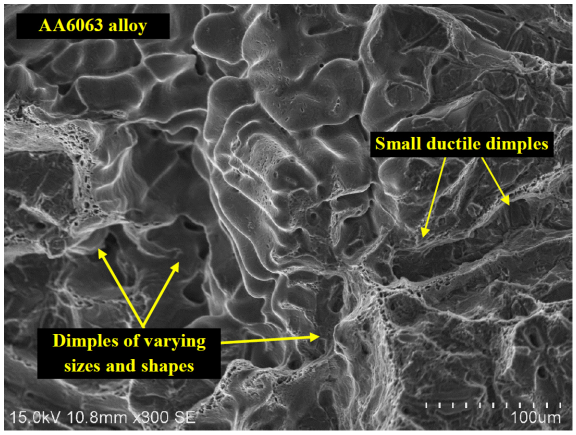

Figure 11. VP-SEM fractography of pure casted AA6063 alloy without added fly ash.

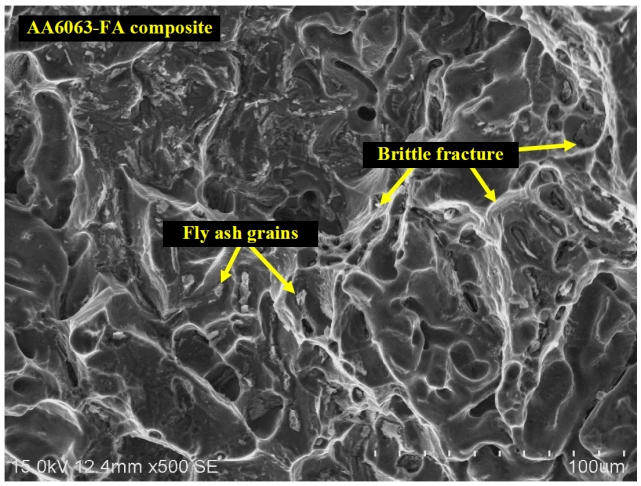

Figure 12. VP-SEM fractography of AA6063-FA composite with 6 wt % fly ash.

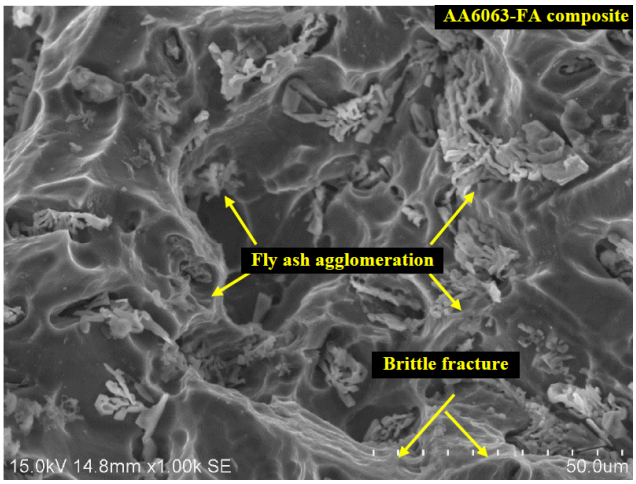

Figure 13. VP-SEM fractography of AA6063-FA composite with 12 wt % fly ash.

5. Conclusions

AA6063-FA composites were successfully fabricated by the compocasting process with different fly ash content. The influence of particulate fly ash reinforcement with AA6063 alloy matrix was investigated. From the XRD results, the mullite and quartz phases was formed from fly ash at 900 °C. The morphology of the fly ash shows that the fly ash particles have a spherical shape with a wide size distribution of particles and smooth surfaces. There are also some non-spherical and non-uniform particles. The bulk density values of casted AA6063-FA composites decrease with an increase in reinforced fly ash particles while the porosity increases. The porosity formation in the AA6063-FA composites can be attributed to the increased content of the fly ash particles, which can lead to an increase in the porosity percentages of composite samples. In this study, the AA6063-FA composite samples with different fly ash content are analyzed using two important mechanical properties, such as Charpy impact testing and microhardness measurements. The value of Charpy impact strength is higher in pure AA6063 alloy samples compared with other percentages of fly ash content composites. The amount of energy absorbed during the fracture decreased steeply with an increasing percentage of fly ash particles in the AA6063 alloy. The Vickers microhardness results of the AA6063-FA composites is higher than that of the pure 6063 alloy. The hardness of composite depends on the hardness of the reinforcement and matrix. The presence of silica and mullite in abundance according to XRD results

increases the brittleness and hardness of aluminum composites when more reinforcing particles of fly ash are added. The fractography of different composite samples reveal some important differences in the appearance of the fractured impact AA6063-FA surfaces with respect to the level of reinforcement The fracture surface of AA6063 alloy without fly ash additives is characterized by the presence of colonies in dimples of varying shapes and sizes, which is an indication that the failure in metal alloy is the result of ductile fracture. When increased the fly ash particles content in the aluminum matrix composites led that to increase the brittleness of aluminum alloy.

Acknowledgments: The authors would like to thank the Aerospace Department in Faculty of Engineering at Universiti Putra Malaysia (UPM) and Mechanical Engineering Faculty, UTM-Centre for Low Carbon Transport, Institute for Vehicle Systems and Engineering at Universiti Teknologi Malaysia (UTM) for providing the research facilities. This research work has been supported by the UPM Research Grant (No. 9463100) and the UTM Research FRGS Grant (No. R.J1300000.7824.4F723).

Author Contributions: Alaa Mohammed Razzaq and Dayang Laila Majid conceived and designed the experiments; Alaa Mohammed Razzaq performed the experiments; Alaa Mohammed Razzaq and Uday M. Basheer analyzed the data; Dayang Laila Majid and Uday M. Basheer contributed reagents/materials/analysis tools; Alaa Mohammed Razzaq wrote the paper and reviewed by Alaa Mohammed Razzaq, Dayang Laila Majid, and Uday M. Basheer and Mohamad R. Ishak.

Conflicts of Interest: The authors declare no conflict of interest.

References

1. Panigrahi, S.K.; Jayaganthan, R. Effect of annealing on precipitation, microstructural stability, and mechanical properties of cryorolled Al 6063 alloy. *J. Mater. Sci.* **2010**, *45*, 5624–5636. [CrossRef]
2. Panigrahi, S.K.; Jayaganthan, R. Development of ultrafine-grained Al 6063 alloy by cryorolling with the optimized initial heat treatment conditions. *Mater. Des.* **2011**, *32*, 2172–2180. [CrossRef]
3. Panigrahi, S.K.; Jayaganthan, R.; Pancholi, V. Effect of plastic deformation conditions on microstructural characteristics and mechanical properties of Al 6063 alloy. *Mater. Des.* **2009**, *30*, 1894–1901. [CrossRef]
4. Al-Fadhalah, K.J.; Almazrouee, A.I.; Aloraier, A.S. Microstructure and mechanical properties of multi-pass friction stir processed aluminum alloy 6063. *Mater. Des.* **2014**, *53*, 550–560. [CrossRef]
5. Li, H.Y.; Zeng, C.T.; Han, M.S.; Liu, J.J.; Lu, X.C. Time-temperature-property curves for quench sensitivity of 6063 aluminum alloy. *Trans. Nonferr. Met. Soc. China* **2013**, *23*, 38–45. [CrossRef]
6. Natarajan, S.; Narayanasamy, R.; Babu, S.K.; Dinesh, G.; Kumar, B.A.; Sivaprasad, K. Sliding wear behaviour of Al 6063/TiB_2 in situ composites at elevated temperatures. *Mater. Des.* **2009**, *30*, 2521–2531. [CrossRef]
7. Nemati, J.; Majzoobi, G.H.; Sulaiman, S.; Baharudin, B.T.H.T.; Hanim, M.A. Effect of equal channel angular extrusion on Al-6063 bending fatigue characteristics. *Int. J. Miner. Metall. Mater.* **2015**, *22*, 395–404. [CrossRef]
8. Sivaprasad, K.; Babu, S.K.; Natarajan, S.; Narayanasamy, R.; Kumar, B.A.; Dinesh, G. Study on abrasive and erosive wear behaviour of Al 6063/TiB_2 in situ composites. *Mater. Sci. Eng. A* **2008**, *498*, 495–500. [CrossRef]
9. Prasad, D.S.; Shoba, C.; Ramanaiah, N. Investigations on mechanical properties of aluminum hybrid composites. *J. Mater. Res. Technol.* **2014**, *3*, 79–85. [CrossRef]
10. Mahendra, K.; Radhakrishna, K. Fabrication of Al-4.5% Cu alloy with fly ash metal matrix composites and its characterization. *Mater. Sci. Pol.* **2007**, *25*, 57–68.
11. Wang, Z.; Georgarakis, K.; Nakayama, K.S.; Li, Y.; Tsarkov, A.A.; Xie, G.; Dudina, D.; Louzguine-Luzgin, D.V.; Yavari, A.R. Microstructure and mechanical behavior of metallic glass fiber-reinforced Al alloy matrix composites. *Sci. Rep.* **2016**, *6*, 24384. [CrossRef] [PubMed]
12. Casati, R.; Vedani, M. Metal matrix composites reinforced by nano-particles—A review. *Metals* **2014**, *4*, 65–83. [CrossRef]
13. Thandalam, S.K.; Ramanathan, S.; Sundarrajan, S. Synthesis, microstructural and mechanical properties of ex situ zircon particles ($ZrSiO_4$) reinforced metal matrix composites (MMCs): A review. *J. Mater. Res. Technol.* **2015**, *4*, 333–347. [CrossRef]
14. Veeravalli, R.R.; Nallu, R.; Mohiuddin, S.M.M. Mechanical and tribological properties of AA7075-TiC metal matrix composites under heat treated (T6) and cast conditions. *J. Mater. Res. Technol.* **2016**, *5*, 377–383. [CrossRef]

15. Rao, V.R.; Ramanaiah, N.; Sarcar, M. Dry sliding wear behavior of Al7075 reinforced with titanium carbide (TiC) particulate composites. In Proceedings of the International Conference on Advances in Materials, Manufacturing and Applications (AMMA 2015), Tiruchirappalli, India, 9–11 April 2015.
16. Allison, J.E.; Cole, G.S. Metal-matrix composites in the automotive industry: Opportunities and challenges. *JOM* **1993**, *45*, 19–24. [CrossRef]
17. Sozhamannan, G.G.; Prabu, S.B.; Venkatagalapathy, V.S.K. Effect of processing parameters on metal matrix composites: Stir casting process. *J. Surf. Eng. Mater. Adv. Technol.* **2012**, *2*, 11.
18. Khosravi, H.; Bakhshi, H.; Salahinejad, E. Effects of compocasting process parameters on microstructural characteristics and tensile properties of A356-SiCp composites. *Trans. Nonferr. Met. Soc. China* **2014**, *24*, 2482–2488. [CrossRef]
19. Shanmughasundaram, P.; Subramanian, R.; Prabhu, G. Some studies on aluminium-fly ash composites fabricated by two step stir casting method. *Eur. J. Sci. Res.* **2011**, *63*, 204–218.
20. Tang, Z.; Chen, X.; Liu, D.; Zhuang, Y.; Ye, M.; Sheng, H.; Xu, S. Experimental investigation of ash deposits on convection heating surfaces of a circulating fluidized bed municipal solid waste incinerator. *J. Environ. Sci.* **2016**, *48*, 169–178. [CrossRef] [PubMed]
21. Barroso, J.; Ballester, J.; Ferrer, L.M.; Jiménez, S. Study of coal ash deposition in an entrained flow reactor: Influence of coal type, blend composition and operating conditions. *Fuel Process. Technol.* **2006**, *87*, 737–752. [CrossRef]
22. Selvam, J.D.R.; Smart, D.R.; Dinaharan, I. Microstructure and some mechanical properties of fly ash particulate reinforced AA6061 aluminum alloy composites prepared by compocasting. *Mater. Des.* **2013**, *49*, 28–34. [CrossRef]
23. Surappa, M. Synthesis of fly ash particle reinforced A356 Al composites and their characterization. *Mater. Sci. Eng. A* **2008**, *480*, 117–124.
24. Guo, R.; Rohatgi, P.; Nath, D. Preparation of aluminium-fly ash particulate composite by powder metallurgy technique. *J. Mater. Sci.* **1997**, *32*, 3971–3974. [CrossRef]
25. Anilkumar, H.; Hebbar, H.; Ravishankar, K. Mechanical properties of fly ash reinforced aluminium alloy (Al6061) composites. *Int. J. Mech. Mater. Eng.* **2011**, *6*, 41–45.
26. Ramachandra, M.; Radhakrishna, K. Synthesis-microstructure-mechanical properties-wear and corrosion behavior of an Al-Si (12%)—Flyash metal matrix composite. *J. Mater. Sci.* **2005**, *40*, 5989–5997. [CrossRef]
27. Efzan, M.E.; Syazwani, N.S.; Abdullah, M.M.A.B. Microstructure and mechanical properties of fly ash particulate reinforced in LM6 for energy enhancement in automotive applications. In *IOP Conference Series: Materials Science and Engineering*; IOP Publishing: Bristol, UK, 2016.
28. Rohatgi, P.K.; Daoud, A.; Schultz, B.F.; Puri, T. Microstructure and mechanical behavior of die casting AZ91D-Fly ash cenosphere composites. *Compos. Part A* **2009**, *40*, 883–896. [CrossRef]
29. Gikunoo, E.; Omotoso, O.; Oguocha, I. Effect of fly ash particles on the mechanical properties of aluminium casting alloy A535. *Mater. Sci. Technol.* **2005**, *21*, 143–152. [CrossRef]
30. Bolton, W. *Engineering Materials Technology*; Elsevier: Amsterdam, The Netherlands, 2013.
31. Bolton, W. *Higher Engineering Science*; Routledge: Abingdon, UK, 2012.
32. Zhou, W.; Xu, Z. Casting of SiC reinforced metal matrix composites. *J. Mater. Process. Technol.* **1997**, *63*, 358–363. [CrossRef]
33. Kok, M. Production and mechanical properties of Al_2O_3 particle-reinforced 2024 aluminium alloy composites. *J. Mater. Process. Technol.* **2005**, *161*, 381–387. [CrossRef]
34. Alaneme, K.; Bodunrin, M. Mechanical behaviour of alumina reinforced AA 6063 metal matrix composites developed by two step-stir casting process. *Acta Tech. Corviniensis Bull. Eng.* **2013**, *6*, 105.
35. Singh, J.; Chauhan, A. Characterization of hybrid aluminum matrix composites for advanced applications—A review. *J. Mater. Res. Technol.* **2016**, *5*, 159–169. [CrossRef]
36. Fan, L.J.; Juang, S.H. Reaction effect of fly ash with Al-3Mg melt on the microstructure and hardness of aluminum matrix composites. *Mater. Des.* **2016**, *89*, 941–949. [CrossRef]
37. Samuel, A.M.; Gotmare, A.; Samuel, F.H. Effect of solidification rate and metal feedability on porosity and SiC-Al_2O_3 particle distribution in an Al-Si-Mg (359) alloy. *Compos. Sci. Technol.* **1995**, *53*, 301–315. [CrossRef]
38. Tekmen, C.; Ozdemir, I.; Cocen, U.; Onel, K. The mechanical response of Al-Si-Mg/SiCp composite: Influence of porosity. *Mater. Sci. Eng. A* **2003**, *360*, 365–371. [CrossRef]

39. Bindumadhavan, P.N.; Chia, T.K.; Chandrasekaran, M.; Wah, H.K.; Lam, L.N.; Prabhakar, O. Effect of particle-porosity clusters on tribological behavior of cast aluminum alloy A356-SiCp metal matrix composites. *Mater. Sci. Eng. A* **2001**, *315*, 217–226. [CrossRef]
40. Surappa, M.; Rohatgi, P. Fluidity of aluminum-silicon-alumina composite. *Metall. Mater. Trans. B* **1981**, *12*, 327–332. [CrossRef]
41. Akhlaghi, F.; Lajevardi, A.; Maghanaki, H.M. Effects of casting temperature on the microstructure and wear resistance of compocast A356/SiCp composites: A comparison between SS and SL routes. *J. Mater. Process. Technol.* **2004**, *155*, 1874–1880. [CrossRef]
42. Mazahery, A.; Shabani, M.O.; Rahimipour, M.R.; Tofigh, A.A.; Razavi, M. Effect of coated B_4C reinforcement on mechanical properties of squeeze cast A356 composites. *Kovove Mater.* **2012**, *50*, 107–113. [CrossRef]
43. Madhusudan, S.; Sarcar, M.M.M.; Rao, N.B.R.M. Mechanical properties of Aluminum-Copper$_{(p)}$ composite metallic materials. *J. Appl. Res. Technol.* **2016**, *14*, 293–299. [CrossRef]
44. Hashim, J.; Looney, L.; Hashmi, M. Particle distribution in cast metal matrix composites—Part II. *J. Mater. Process. Technol.* **2002**, *123*, 258–263. [CrossRef]
45. Nishida, Y. *Introduction to Metal Matrix Composites: Fabrication and Recycling*; Springer Science & Business Media: Berlin, Germany, 2013.
46. Srivastava, A.K.; Das, K. Microstructural and mechanical characterization of in situ TiC and (Ti, W)C-reinforced high manganese austenitic steel matrix composites. *Mater. Sci. Eng. A* **2009**, *516*, 1–6. [CrossRef]
47. Basak, A.; Pramanik, A.; Islam, M.N.; Anandakrishnan, V. Challenges and recent developments on nanoparticle-reinforced metal matrix composites. In *Fillers and Reinforcements for Advanced Nanocomposites*; Elsevier Science & Technology: Amsterdam, The Netherlands, 2015; p. 349.